Resonant oscillations of atmospheric neutrinos with an underground muon detector

G. Auriemma
Physics Department, Boston University, Boston, Massachusetts 02215
and INFN Sezione di Roma, Rome, Italy

M. Felcini
Physics Department, Boston University, Boston, Massachusetts 02215

P. Lipari
INFN Sezione di Roma, Rome, Italy

J. L. Stone
Physics Department, Boston University, Boston, Massachusetts 02215
(Received 8 June 1987)

We have reanalyzed the sensitivity of an underground muon detector to $(\nu_\mu \leftrightarrow \nu_e)$ oscillations, taking into account the Wolfenstein, Mikheyev, and Smirnov matter effect. We find that the measurement of the charge of the muons would greatly improve the sensitivity of this type of experiment. Such a measurement would enhance the statistical significance of an eventual oscillation signal and, allowing for a comparison of the μ^- and μ^+ fluxes, can eliminate the systematic uncertainty upon the absolute normalization of the neutrino flux. We show that a realistic detection system can explore the region in parameter space $3\times10^{-3} \leq \Delta m^2 \leq 10^{-1}$ eV^2 and $\sin^2 2\theta \geq 0.02$, which is well below current accelerator and reactor limits.

I. INTRODUCTION

Since the original suggestion by Pontecorvo[1] of the possibility of neutrino oscillations, a large amount of theoretical and experimental work has gone into the study of this problem. A search was proposed for neutrino oscillations using the flux of neutrinos produced in the atmosphere by the interaction of primary cosmic rays with air nuclei, via the subsequent decay of π's, K's, and μ's. In fact, the neutrinos reaching a detector located near Earth's surface have traveled a distance (ψ is the nadir angle) $x = 2R_\oplus \cos\psi$, or $\sim 10^4$ km; neutrino-oscillation lengths of this order become therefore experimentally accessible. This experimental method is very appealing in principle, but suffers from several limitations. First, the flux of atmospheric neutrinos is small, so that the sensitivity of even a very large detector is seriously limited by statistics. The flux is also a mixture of ν_e, $\bar{\nu}_e$, ν_μ, and $\bar{\nu}_\mu$ in proportions which depend upon the neutrino energy and direction. Furthermore, the absolute intensities can be predicted with an accuracy estimated to be of the order of $\sim 20\%$, due to the uncertainties upon the primary-cosmic-ray flux and upon the hadronic topological cross sections at very high energies. Geomagnetic and solar-wind effects are additional sources of errors in a precise calculation of the low-energy part of the neutrino flux.

In large proton-decay detectors, such as the IMB (Irvine-Michigan-Brookhaven) or Kamiokande detectors, these difficulties can be partially circumvented by comparing the rates of showering neutrino interactions, which are attributed to ν_e or $\bar{\nu}_e$, to the muon-neutrino interactions inside the detector volume. A difference in this ratio among the upward-going neutrinos and the downward-going ones could be interpreted as a signal for oscillations.[2]

In this paper we will concentrate on a different approach, consisting of the indirect measure of the ν_μ (or $\bar{\nu}_\mu$) flux through the detection of muons produced by charged-current interactions in the rock underneath the detector. The event rate is expected to be larger then in proton-decay detectors because a larger target mass is available for neutrino interactions. Analysis of the sensitivity of an underground muon detector to neutrino oscillations have already been published,[3] but most of the results were obtained using the vacuum oscillation probability; hence the effect of the presence of matter along the neutrino path was neglected.

It is well known that a neutrino produced as a ν_μ has a probability

$$P^{(\mathrm{vac})}_{\nu_\mu \to \nu_\mu} = P^{(\mathrm{vac})}_{\bar{\nu}_\mu \to \bar{\nu}_\mu} = 1 - \tfrac{1}{2}\sin^2 2\theta \left[1 - \cos\left(\frac{\Delta m^2}{E} R_\oplus \cos\psi \right) \right] \quad (1)$$

of emerging with the same flavor, crossing an "empty" Earth, if θ is the mixing angle and $\Delta m^2 = m_2^2 - m_1^2$ the mass splitting. But Wolfenstein[4] and Mikheyev and Smirnov[5] have shown that in the presence of matter the neutrino-oscillation picture changes dramatically. It was shown qualitatively by Wolfenstein that for maximal or nearly maximal mixing (viz., $\sin^2 2\theta \simeq 1$) the matter effect reduces the oscillation probability. On the contrary Mikheyev and Smirnov have shown that, for a small mixing angle, the transition probability has a resonance at the energy

$$\Delta m^2 \cos 2\theta = 2\sqrt{2} G_F E n_e \ , \tag{2}$$

where G_F is the Fermi constant and n_e is the electron number density.

In order to have a large resonant effect, however,

$$l_{\rm osc}(\text{res}) = \frac{4\pi E}{\Delta m^2 \sin^2 2\theta} = \frac{\sqrt{2}\pi}{G_F n_e} \frac{\cos 2\theta}{\sin^2 2\theta} \sim 4R_\oplus \ , \tag{3}$$

which corresponds to the requirement of a neutrino-oscillation length at a resonance comparable with Earth's diameter. The need of the condition expressed by the formula (3) is physically transparent if we consider that if $l_{\rm osc}(\text{res})$ is much larger than $4R_\oplus$, the oscillations do not have time to grow and there will be little or no transition at all.

Neutrinos that satisfy both conditions (2) and (3) will emerge, from the Earth, nearly entirely rotated into the mixed flavor. If the neutrino masses are ordered in the "natural" way, namely, if the lightest neutrino is a mixture made up predominantly of ν_e ($\Delta m^2 > 0$), the resonant transition takes place for neutrinos only, whether or not the transition probability for antineutrinos is even reduced, compared to the vacuum case. On the contrary, if the masses are ordered in the opposite way ($\Delta m^2 < 0$), the role of ν and $\bar{\nu}$ are exchanged, or, viz., antineutrino transitions are enhanced and neutrino transitions reduced.

Resonant neutrino oscillations could explain[6] the low capture rate of solar neutrinos registered by the Davis experiment.[7] In the following we are going to discuss quantitatively the above-outlined scenario.

II. NEUTRINO OSCILLATIONS IN MATTER

In ordinary matter, electron neutrinos have one extra type of interaction, in respect to the other neutrino flavors, due to the charged-current elastic scattering on electrons. The extra interaction term is equivalent to the existence of an additional effective potential for ν_e (Ref. 4) (the positive sign is crucial):

$$V = +\sqrt{2} G_F n_e \ , \tag{4}$$

where G_F is the Fermi constant and n_e is the electron density. Using the relationship

$$(E - V) = \sqrt{p_\nu^2 + m^2} \simeq p_\nu + \frac{m^2}{2p_\nu} \tag{5}$$

we can see that the presence of matter is equivalent to adding to the square of the mass of the electron neutrino an extra positive contribution

$$A = \delta m_e^2 = 2p_\nu V = 2\sqrt{2} G_F n_e p_\nu \ , \tag{6}$$

where $n_e = \rho Y_e / m_N$, ρ being the mass density, Y_e the number of electrons per nucleon, and m_N the nucleon mass. Taking $Y_e = \frac{1}{2}$, and measuring ρ in g cm^{-3} and p_ν in GeV, we have numerically

$$A = 0.76 \times 10^{-4} \rho p_\nu \ \text{eV}^2 \ . \tag{7}$$

An electron neutrino of momentum 1 GeV at the center of the Earth ($\rho \simeq 12 \ \text{g cm}^{-3}$) would have its mass raised by $\sim 10^{-3}$ eV^2. In the case of an electron antineutrino the effective potential has the opposite sign; hence, the $\bar{\nu}_e$ get a negative contribution to their squared mass.

If neutrinos have mass, the flavor eigenstates $|\nu_\alpha\rangle$ will be a linear superposition of mass eigenstates $|\nu_j\rangle$ with a general form

$$|\nu_\alpha\rangle = \sum_j U_\alpha^j |\nu_j\rangle \ , \tag{8}$$

where U is a unitary matrix with rank equal to the number of neutrino flavors. Antineutrino states will also be a linear superposition of mass eigenstates with a mixing matrix $\bar{U} = U^*$. The matter effect will modify the eigenvalues and eigenvectors of effective squared-mass operator: $\hat{M}^2_{\rm eff} = \hat{M}^2 \pm A\hat{P}_e$, where $\hat{P}_e$ is the electron-neutrino projection operator and A is given by formula (6). Obviously the new eigenstates of mass will be different for neutrinos and antineutrinos.

In the case of two flavors, the mixing matrix depends on a single angle θ that can be chosen in the interval ($0 \le \theta \le \pi/2$) and the eigenvalues can easily be found. If $\Delta m^2 = m_2^2 - m_1^2$ is the mass splitting in a vacuum, the splitting for neutrinos of energy E in matter with electron density n_e will be

$$(\Delta m^2)_{\rm eff} = [(\Delta m^2 \cos 2\theta \mp 2\sqrt{2} G_F n_e E)^2 + (\Delta m^2 \sin 2\theta)^2]^{1/2} \ , \tag{9}$$

where the minus sign holds for neutrinos and the plus sign for antineutrinos. The effective mixing angle in matter θ_m becomes

$$\sin^2 2\theta_m = \frac{(\Delta m^2 \sin 2\theta)^2}{(\Delta m^2 \cos 2\theta \mp 2\sqrt{2} G_F n_e E)^2 + (\Delta m^2 \sin 2\theta)^2} \ . \tag{10}$$

We can see that if $\Delta m^2 > 0$ at the resonance, the two neutrino flavors are degenerate in mass $[(\Delta m^2)_{\rm eff} = 0]$ and are fully mixed ($\sin^2 2\theta_m = 1$). We therefore expect large transition probabilities for neutrinos that during their trajectory cross a layer of matter for which the condition (2) is satisfied. The same would happen for antineutrinos if $\Delta m^2 < 0$.

To compute the flavor evolution of a neutrino of a given energy traveling across matter with variable electron density $n_e(x)$, we have to integrate, with suitable initial conditions, the Schrödinger equation

$$i\frac{d}{dx} |\nu(x)\rangle = \hat{H}_{\rm eff}(x) |\nu(x)\rangle \ , \tag{11}$$

where $\hat{H}_{\rm eff}$ is the effective Hamiltonian operator, viz., $\hat{H}_{\rm eff} \simeq \hat{M}^2_{\rm eff}/2E + \hat{p}$. Neglecting an irrelevant trace part, we have, for two neutrino flavors,

$$i\frac{d}{dx}\begin{bmatrix}\nu_e(x)\\ \nu_\mu(x)\end{bmatrix}=\frac{1}{4E}\begin{bmatrix}A(x)-\Delta m^2\cos2\theta & \Delta m^2\sin2\theta\\ \Delta m^2\sin2\theta & -A(x)+\Delta m^2\cos2\theta\end{bmatrix}\begin{bmatrix}\nu_e(x)\\ \nu_\mu(x)\end{bmatrix}. \tag{12}$$

The flavor-evolution equation for antineutrinos can be obtained reversing the sign of the matter contribution in the diagonal terms of the matrix. In the case of two neutrino flavors we have trivially, from unitarity,

$$P_{\nu_e\to\nu_e}=P_{\nu_\mu\to\nu_\mu}=1-P_{\nu_e\to\nu_\mu}=1-P_{\nu_\mu\to\nu_e}\,, \tag{13}$$

$$P_{\bar\nu_e\to\bar\nu_e}=P_{\bar\nu_\mu\to\bar\nu_\mu}=1-P_{\bar\nu_e\to\bar\nu_\mu}=1-P_{\bar\nu_\mu\to\bar\nu_e}\,. \tag{14}$$

III. NEUTRINO OSCILLATIONS IN THE EARTH

To study $(\nu_e\leftrightarrow\nu_\mu)$ oscillations in the Earth, we have numerically integrated the system of differential equations (12), taking into account the variable density of the Earth and assuming the initial conditions corresponding to a pure-flavor state ($|\nu_e\rangle$ or $|\nu_\mu\rangle$).

We have performed this integration using a Runge-Kutta method, including a density distribution taken from Ref. 8, which is also plotted in Fig. 1. The relevant feature, from the point of view of neutrino oscillations, is the existence of two distinct regions, namely, the core and the mantle, separated by a sharp density discontinuity at a radius of $\sim$2800 km. In the core the density varies, from $\rho\simeq12.5$ g cm^{-3} to $\rho=9.9$ g cm^{-3}. At the sharp boundary between core and mantle, the density jumps down to ~5.5 g cm^{-3}, and decreases rather smoothly with the radius, reaching the average density of standard rock $\rho\sim2.8$ g cm^{-3} at the surface.

A typical result obtained from the integration of (12) is shown in Fig. 2(a), where the probability $P_{\nu_\mu\to\nu_\mu}$ for a vertical upward-going ($\psi=0°$) neutrino crossing the Earth is plotted as a function of the adimensional ratio $E/\Delta m^2$. This was obtained by fixing the mixing angle equal to the Cabibbo angle ($\sin^2 2\theta=0.04$). In Fig. 2(b) we have reported the same probability for antineutrinos and, for comparison, in Fig. 2(c) we have plotted the values obtained from formula (1), viz., the survival probability in vacuum. We see in this figure that resonant conversion of neutrinos take place only for two rather narrow ranges of energies, if we fix the value of the mass splitting. Those two energies correspond to the values which satisfy condition (2), respectively, in the core or in the mantle. As can be checked from the same formula, the values of those two energies are given approximately by

$$E_\nu(\text{core})\simeq(1.0-1.3)\left[\frac{\Delta}{10^{-3}\ \text{eV}^2}\right]\cos2\theta\ \text{GeV}\,, \tag{15}$$

$$E_\nu(\text{mantle})\simeq(2.3-4.7)\left[\frac{\Delta}{10^{-3}\ \text{eV}^2}\right]\cos2\theta\ \text{GeV}\,. \tag{16}$$

Qualitatively we expect, for those particular energies, to have a nearly complete suppression of the original neutrino flavor; on the contrary the oscillation probability for antineutrinos is even smaller than in a vacuum. This

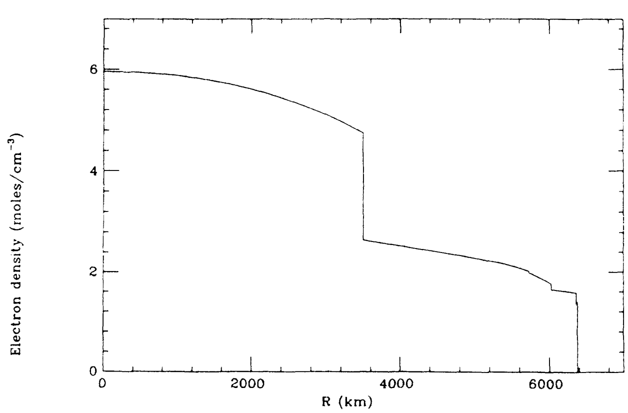

FIG. 1. Electron density inside the Earth as a function of the radius. The data is taken from Ref. 8.

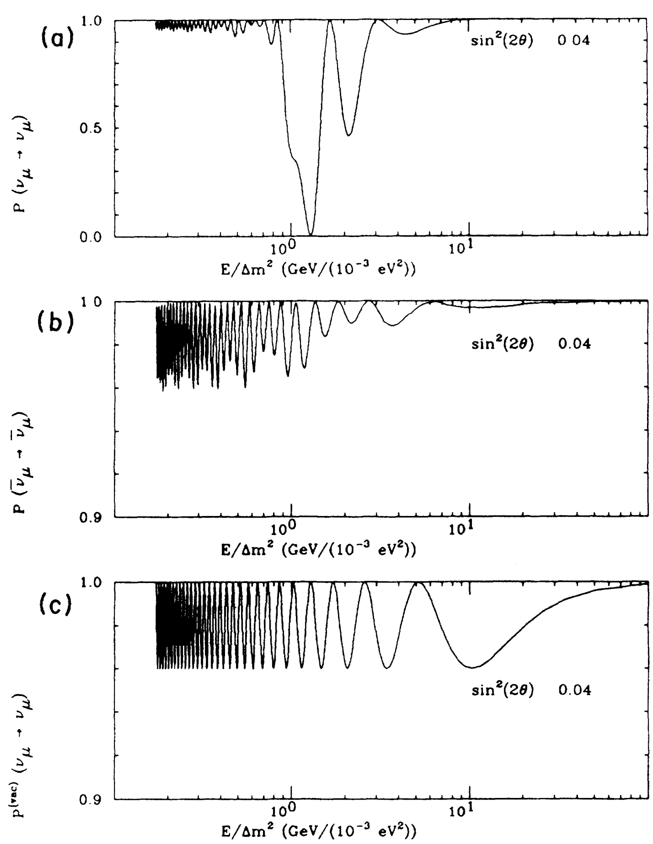

FIG. 2. Diagonal transition probability for vertical neutrinos ($\psi=0°$) as a function of $E/\Delta m^2$ for a fixed value of the mixing parameter ($\sin^2 2\theta=0.04$) that corresponds roughly to the Cabibbo angle. (a) shows the transition probability for neutrinos (assuming $\Delta m^2>0$), (b) for antineutrinos. (c) gives for comparison the transition probability obtained neglecting the matter effect.

is a very interesting result, which suggests a definite signature for the oscillation signal in atmospheric neutrinos. In fact, as we will discuss later, the atmospheric neutrinos are distributed over a rather large energy range and consist of a mixture of neutrinos and antineutrinos; therefore, if we could distinguish the leptonic charge of the detected neutrinos, the oscillation signal would manifest itself as a variation of the ratio $\nu/\bar{\nu}$ versus energy.

In Fig. 3 we show the survival probabilities $P_{\nu_\mu\to\nu_\mu}$ for different inclinations of the neutrino beam. When $\psi \geq 32°$, neutrinos entirely miss the core and the resonant transition is possible in the mantle for neutrino energies given by (16). In Fig. 4 the same quantity is shown for several values of the mixing parameter $\sin^2 2\theta$. We observe that resonant conversion in the Earth can occur for mixing angles $\sin^2 2\theta \geq 0.01$.

Until now we have considered the mixing of two flavors only, but we know that there are at least three neutrino flavors. In this case the mixing matrix can be parametrized by three angles and a CP-violating phase. The most convenient parametrization is the one suggested by Maiani,[9] in the form

$$U = \mathrm{diag}(1,1,e^{-i\delta})\exp(i\lambda_7\theta_{e\tau})\mathrm{diag}(1,1,e^{+i\delta}) \times \exp(i\lambda_5\theta_{\mu\tau})\exp(i\lambda_2\theta_{e\mu}) , \tag{17}$$

where the λ's are the Gell-Mann matrices. If the three neutrino masses are well separated and the three mixing angles are small (as for example in the scenario predicted by the seesaw model of Gell-Mann, Ramond, and Slansky[10]), it is easy to see that we expect two well-separated resonances.

Assuming that the neutrino masses are ordered in a natural way (i.e., like the ones of the corresponding charged leptons) for

$$E_\nu \simeq \frac{m_2^2 - m_1^2}{2\sqrt{2}G_F n_e} , \tag{18}$$

ν_e and ν_μ will be fully mixed (with only a small contam-

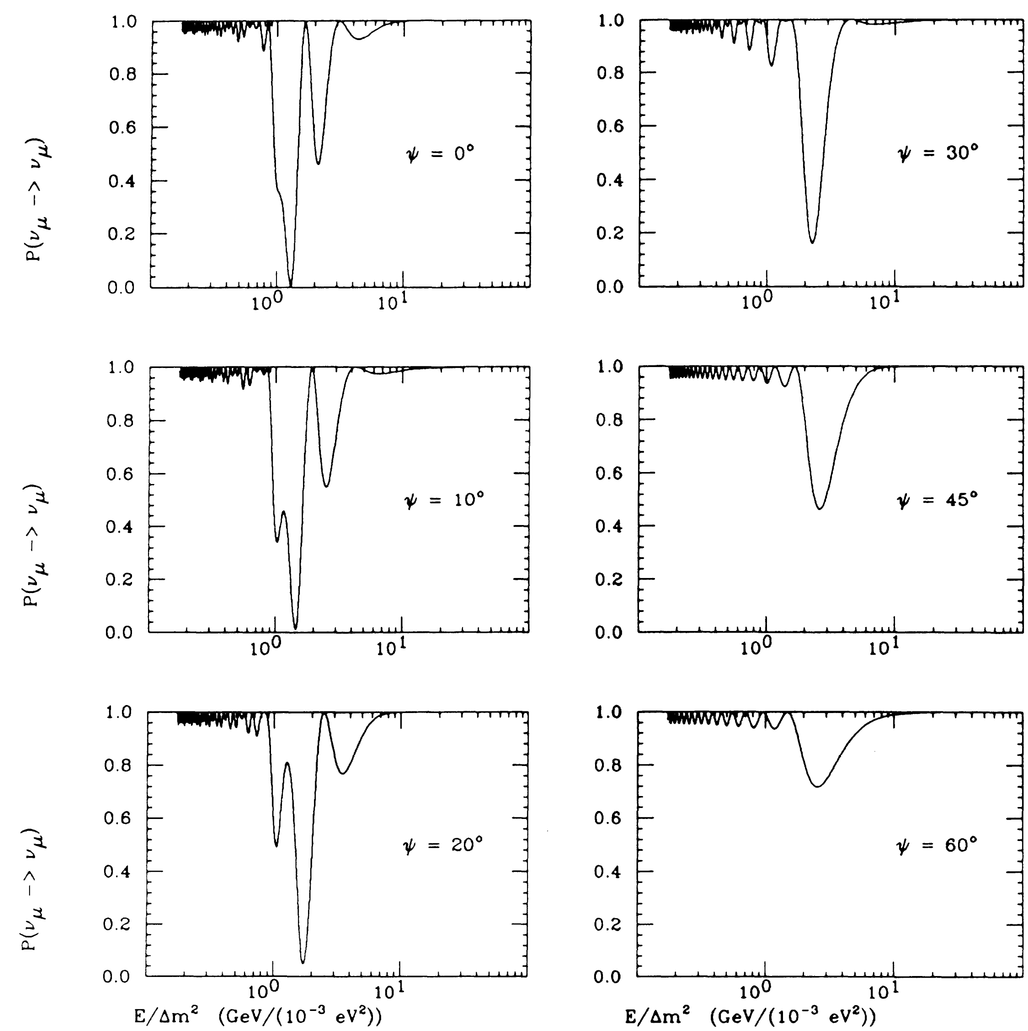

FIG. 3. Diagonal transition probability $P_{\nu_e\to\nu_e} = P_{\nu_\mu\to\nu_\mu}$ as a function of $E/\Delta m^2$ for a fixed value of the mixing parameter ($\sin^2 2\theta = 0.04$) and different values of the nadir angle (ψ=0°, 10°, 20°, 30°, 45°, and 60°). For angles $\psi < 32°$ the transition probability has two peaks corresponding to resonances in the Earth core and in the Earth mantle. For $\psi > 32°$, only the mantle resonance is present.

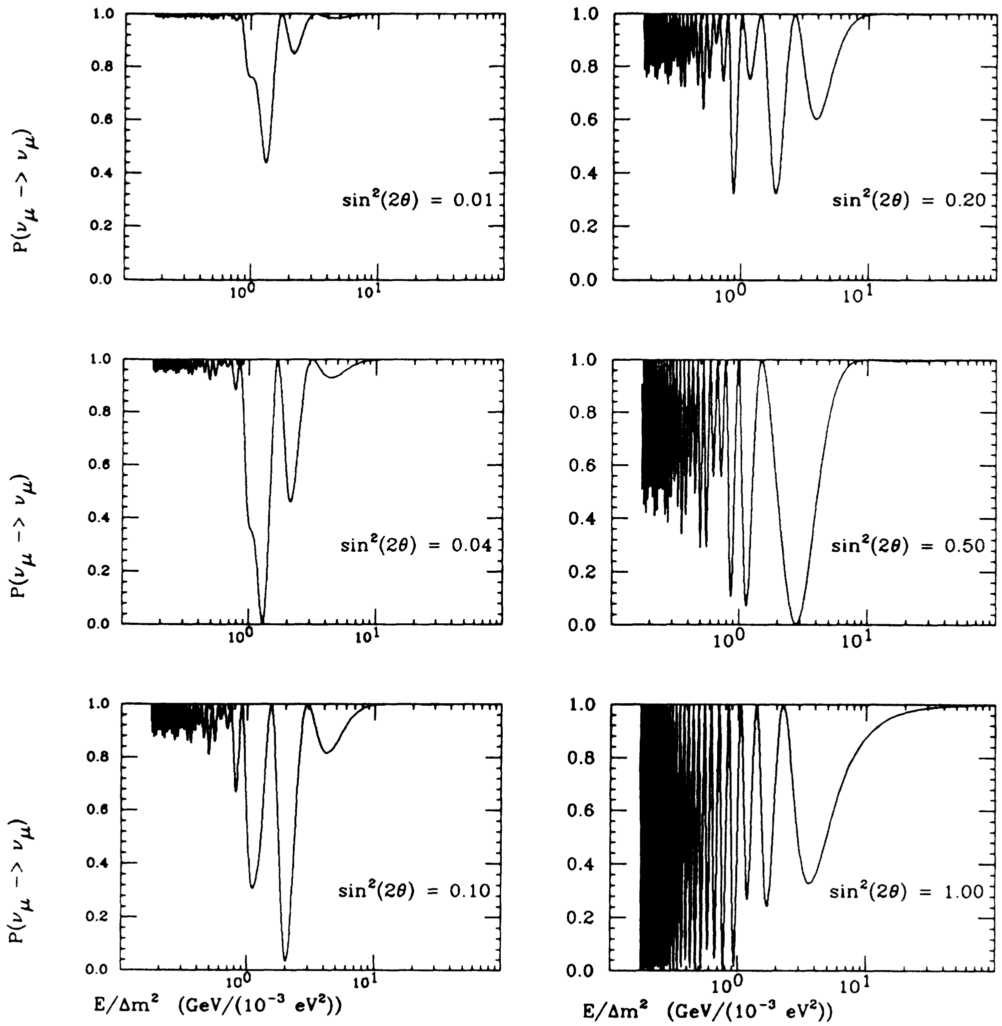

FIG. 4. Diagonal transition probability as a function of $E/\Delta m^2$ for vertical neutrinos ($\psi=0°$). The different curves correspond to different values of the mixing parameter ($\sin^2 2\theta=0.01$, 0.04, 0.10, 0.20, 0.50, 1).

ination of ν_τ). Alternatively, when the neutrino energy satisfies

$$E_\nu \simeq \frac{m_3^2-m_1^2}{2\sqrt{2}G_F n_e} , \tag{19}$$

ν_e and ν_τ will be fully mixed (with only a small contamination of ν_μ). In both cases, as shown by Kuo and Pantaleone,[11] we can neglect the small contamination due to the extra neutrino flavor and use the results obtained in the two flavor case by just inserting the appropriate mixing parameter, i.e., $\sin^2 2\theta_{e\mu}$ for the lower-energy ($\nu_e \leftrightarrow \nu_\mu$) transition, and $\sin^2 2\theta_{e\tau}$ for the higher-energy ($\nu_e \leftrightarrow \nu_\tau$) transition. It is worth noticing, anyhow, that in the two extreme cases of nearly degenerate neutrino masses or large mixing angles, the general solution might be quite different.

IV. THE FLUX OF NEUTRINO-INDUCED UPWARD MUONS

The predicted spectrum of neutrinos at the detector, once that we have assigned the values of Δm^2 and $\sin^2 2\theta$, will be given by the formula

$$\frac{d^2\phi_{\nu_\mu}^{\rm det}}{d\Omega\, dE} = [1-P(E_\nu,\psi)]\frac{d^2\phi_{\nu_\mu}}{d\Omega\, dE}(E_\nu,\psi) + P(E_\nu,\psi)\frac{d^2\phi_{\nu_e}}{d\Omega\, dE}(E_\nu,\psi) . \tag{20}$$

The spectrum of antineutrinos will be

$$\frac{d^2\phi_{\bar\nu_\mu}^{\rm det}}{d\Omega\, dE} = [1-\bar P(E_{\bar\nu},\psi)]\frac{d^2\phi_{\bar\nu_\mu}}{d\Omega\, dE}(E_{\bar\nu},\psi) + \bar P(E_{\bar\nu},\psi)\frac{d^2\phi_{\bar\nu_e}}{d\Omega\, dE}(E_{\bar\nu},\psi) , \tag{21}$$

where $\bar P$ is the survival probability for $\bar\nu$ defined above.

As a signal of neutrino resonant conversion, we suggest a search for a suppression of neutrinos relative to the antineutrinos. This method is free of any bias if the ratio $\nu/\bar\nu$ is constant. We have used, in the following analysis, an accurate and reliable tabulation of neutrino fluxes, from 1 to 10^6 GeV, calculated by Volkova.[12] The ratio $\nu/\bar{\nu}$, given in the latter paper for few points only, is slowly variable both with the energy and with the angle ψ. Hence a more refined analysis should take into account a small "second-order" effect, due to this variability. We have neglected this correction, inserting in our computations a constant ratio $\nu_\mu/\bar{\nu}_\mu=1.2$ and $\nu_e/\bar{\nu}_e=1.2$. We remark that the present uncertainty on this ratio can be eliminated by direct experimental measurements of the muon's charge ratio; therefore, it is not to be considered an intrinsic limitation to the search for oscillation with this method.

Following the analytical method of Gaisser and Stanev[13] we have computed the flux of upward muons, folding the neutrino spectrum with the interaction cross section and taking into account the energy loss of muons in rock. We define the differential yield dY/dE_μ as the number of muons per unit energy E_μ produced by a neutrino (or antineutrino) of energy E_ν, given by

$$\frac{dY^{\mp}}{dE_\mu}(E_\mu,E_\nu)=N_A\int_0^\infty dX\int_{E_\mu}^{E_\nu}dE\frac{d\sigma_{\nu(\bar{\nu})}}{dE}(E,E_\nu)\times\frac{dp_{\rm surv}}{dE_\mu}(E_\mu;E,X)\ , \tag{22}$$

where X will be the distance to the interaction point, E the energy of the muon at this point, N_A is the Avogadro number, $d\sigma/dE$ the differential cross section, and $dp_{\rm surv}/dE_f(E_f,E_i,X)$ is the probability that a μ of initial energy E_i will cross a thickness of material X emerging with energy E_f. It is obvious that Y^- is the yield for neutrinos and Y^+ the one for antineutrinos.

Formula (22) can be simplified by neglecting the fluctuations in muon energy loss. In this limit, approximating the average energy loss with the functional form $dE/dX=a(1+E/\epsilon)$, we find

$$\frac{dp_{\rm surv}}{dE_\mu}(E_f,E_i,X)=\delta(E_f-E_{\rm out}(E_i,X))=\frac{\delta(X-X_0(E_i,E_f))}{a(1+E/\epsilon)}\ , \tag{23}$$

where

$$X_0=\frac{\epsilon}{a}\ln\left[\frac{E_i+\epsilon}{E_f+\epsilon}\right]. \tag{24}$$

Integrating over X and introducing the standard variable, $y=1-E_\mu/E_\nu$, we find

$$\frac{dY^{\mp}}{dE_\mu}(E_\mu,E_\nu)=N_A\frac{1}{a(1+E/\epsilon)}\times\int_0^{1-E_\mu/E_\nu}dy\frac{d\sigma_{\nu(\bar{\nu})}}{dy}(y,E_\nu)\ . \tag{25}$$

The differential flux of muons produced by neutrinos is obtained by folding the neutrino spectrum with the muon differential yield

$$\frac{d^2\Phi_{\mu^\mp}}{dE_\mu}(E_\mu,\Omega)=\int_{E_\mu}^\infty dE_\nu\frac{d^2\Phi^{\rm det}_{\nu_\mu(\bar{\nu}_\mu)}}{dE_\nu d\Omega}(E_\nu,\Omega)\times\frac{dY^{\mp}}{dE_\mu}(E_\mu,E_\nu)\ , \tag{26}$$

The yields were estimated taking into account the cross section of deep-inelastic scattering of neutrinos, and neutrinos only, which, in the usual formalism of the QCD parton model, is

$$\frac{d^2\sigma_\nu}{dx\,dy}=\frac{G_F^2 s}{2\pi}\left[\frac{M_W^2}{Q^2+M_W^2}\right]^2\{[d(x)+s(x)]+(1-y)^2[\bar{u}(x)+\bar{c}(x)]\}\ , \tag{27}$$

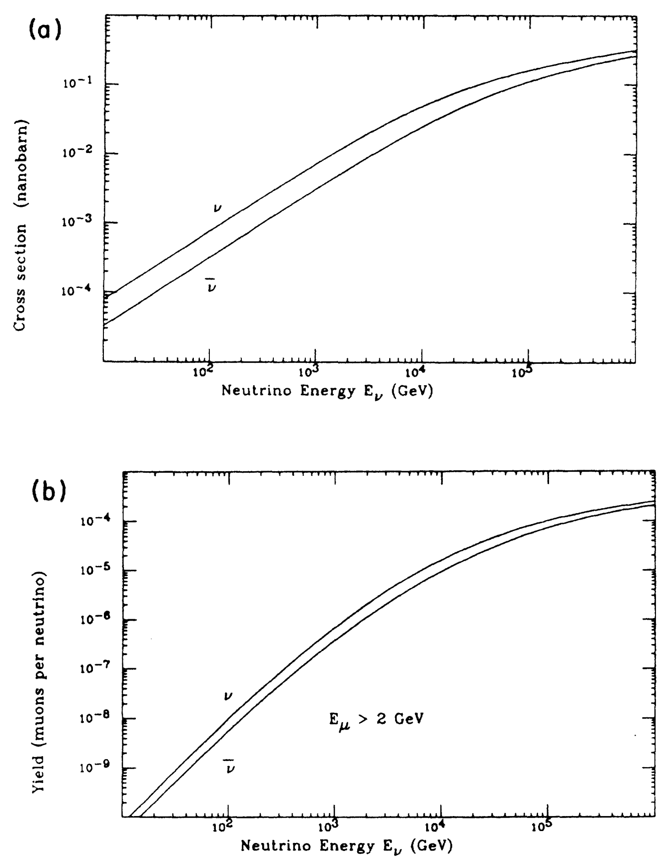

FIG. 5. (a) shows the cross section per nucleon $\sigma_\nu(E)$ and $\sigma_{\bar{\nu}}(E)$ of the inclusive charged-current reactions $\nu_\mu+N\rightarrow\mu^-+X$ and $\bar{\nu}_\mu+N\rightarrow\mu^++X$ as a function of neutrino energy. (b) shows the integrated yield $Y^{\pm}(E)$ [cf. Eq. (29) in the text] or the number of μ^- (μ^+) with energy $E_\mu\geq 2$ GeV produced by a ν_μ ($\bar{\nu}_\mu$) of energy E.

$$\frac{d^2\sigma_{\bar{\nu}}}{dx\,dy}=\frac{G_F^2 s}{2\pi}\left[\frac{M_W^2}{Q^2+M_W^2}\right]^2\{(1-y)^2[u(x)+c(x)]+[\bar{d}(x)+\bar{s}(x)]\}\ .$$

We have considered an isoscalar target and used the parametrization of quark distributions calculated from QCD by Duke and Owens.[14] (We neglect here the quasielastic channels. The contribution to the rate of upward-going muons given by these channels is important at low energies, but it is a small correction only for energies $E_\mu \geq 2$ GeV, considered here.) The cross section $\sigma_\nu(E)$ $[\sigma_{\bar{\nu}}(E)]$ for neutrino interactions on an isoscalar target are shown in Fig. 5(a). We reproduce accurately the low-energy linear rise, and the flattening around $2mE \sim M_W^2$ when the W-propagator terms become important. The ratio $\sigma_\nu/\sigma_{\bar{\nu}}$ is ~ 3 at low energies and then slowly decreases and tends to 1 for very large energies when the cross section becomes a δ function $\sigma_\nu \simeq \sigma_{\bar{\nu}} \simeq \sigma_0(E)\delta(y)$.

The integrated yield

$$Y^{\pm}(E_\nu;E_{\min})=\int_{E_{\min}}^{E_\nu} dE\frac{dY^{\pm}}{dE}(E,E_\nu) \tag{28}$$

is shown in Fig. 5(b) for $E_{\min}=2$ GeV. At low energies $Y(E_\nu)$ grows quadratically because of the linear increase of the cross section and the muon range. At high energies $Y(E_\nu)$ grows logarithmically with energy. The ratio Y^-/Y^+ is approximately 2 at low energies. The total cross sections are in a ratio ~ 3, but the antineutrino differential cross section with a dominant behavior $\sim(1-y)^2$ is harder than the neutrino one (flat in y). Finally we plot in Fig. 6 the differential spectrum of positive and negative muons for the vertical $\psi=0°$ and the

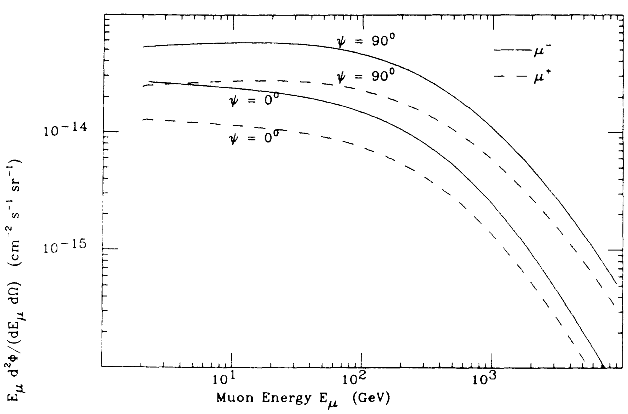

FIG. 6. Differential flux $[d^2\phi_\mu^{\pm}/(d\ \ln E_\mu d\Omega)]$ of upward μ's for the two values of nadir angles $\psi=0°$ and $\psi=90°$. The flux is approximately of form $\sim 1/E_\mu$. The horizontal flux is larger than the vertical flux by a factor $\simeq 2$. The μ^- flux is about twice the μ^+ flux.

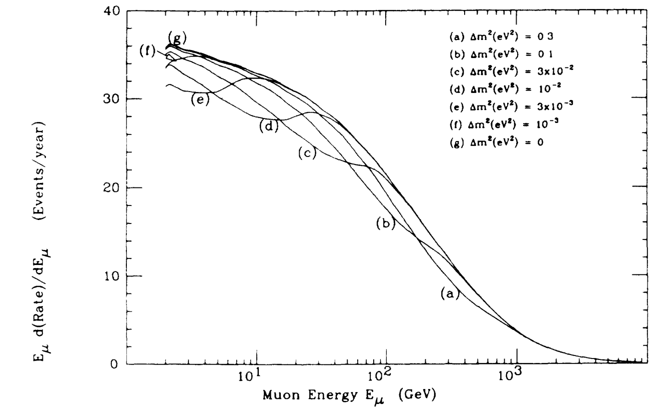

FIG. 7. Differential rate of upward μ^- as a function of energy integrated over nadir angles $(0° \leq \psi \leq 60°)$. The different curves describe the expected rates without neutrino oscillations, and assuming a mixing parameter $\sin^2 2\theta=0.04$ and different values of the mass difference Δm^2. For different values of Δm^2 the rate is depleted in different energy regions.

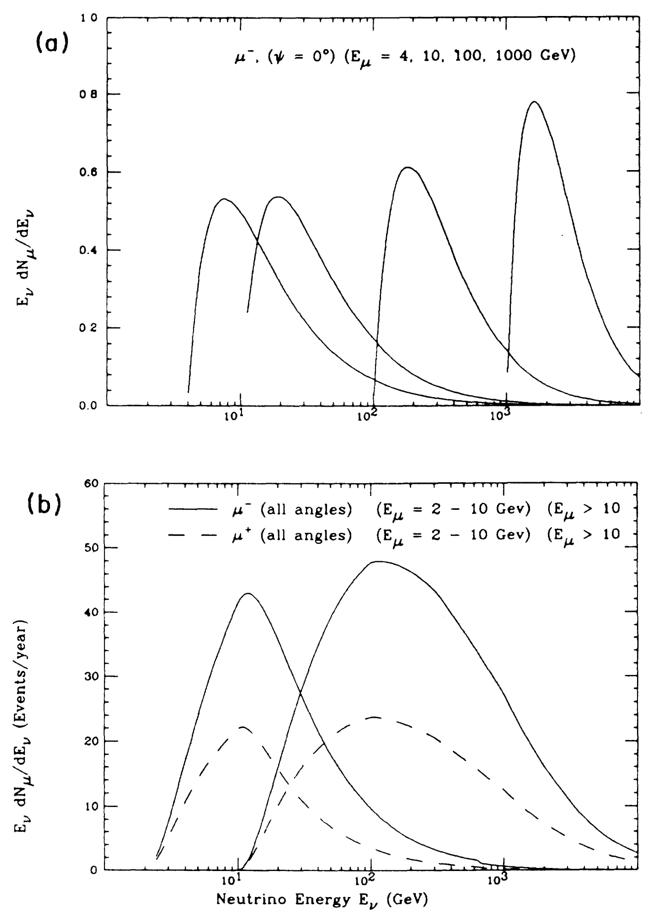

FIG. 8. (a) shows the shape of the μ^- flux produced by a neutrino of fixed energy $E_\nu=4$, 10, 100, and 1000 GeV. (b) shows the spectrum of neutrinos that produce μ's in the detector. The different curves are for ν_μ and $\bar{\nu}_\mu$, and for two energy regions of the μ's, 2 GeV $\leq E_\mu \leq 10$ GeV and $E_\mu \geq 10$ GeV.

horizontal $\psi=90°$ directions.

Integrating the muon flux over the energy region ($E_\mu \geq 2$ GeV), and over two different angular regions we find

$$\phi_{\mu^-}(0° \leq \psi \leq 60°)=0.39\times 10^{-12}\ \mathrm{cm}^{-2}\mathrm{s}^{-1}\ , \tag{29}$$

$$\phi_{\mu^-}(60° \leq \psi \leq 90°)=0.64\times 10^{-12}\ \mathrm{cm}^{-2}\mathrm{s}^{-1}\ , \tag{30}$$

$$\phi_{\mu^+}(0° \leq \psi \leq 60°)=0.19\times 10^{-12}\ \mathrm{cm}^{-2}\mathrm{s}^{-1}\ , \tag{31}$$

$$\phi_{\mu^+}(60° \leq \psi \leq 90°)=0.31\times 10^{-12}\ \mathrm{cm}^{-2}\mathrm{s}^{-1}\ . \tag{32}$$

Summing the negative and positive muon flux, we obtain a result in excellent agreement with Ref. 13. We can see that μ^+ flux is about a factor 2 smaller than the μ^- flux, because of the smaller yield of $\bar{\nu}_\mu$. The horizontal flux is also larger than the vertical flux because of the well known enhancement at large zenith angles.

To estimate the sensitivity of a real experiment, we have to translate these fluxes into event rates. The rate of upward-going muons in the solid angle $\Delta\Omega$ in a fully sensitive detector (i.e., neglecting dead zones and triggering and reconstruction inefficiencies) is given by the formula

$$R=t\int_{\Delta\Omega} d\Omega\, S(\psi,\phi)\int_{E_{\min}}^{E_{\max}} dE_\mu \frac{d^2\Phi_\mu}{dE_\mu d\Omega}(E_\mu,\Omega)\ , \tag{33}$$

where $S(\psi,\phi)$ is the detector area projected onto a plane perpendicular to the direction (ψ,ϕ). For the simple geometry of a parallelepiped we have

$$S(\psi,\phi)=(S_x\,|\cos\phi\,|+S_y\,|\sin\phi\,|\,)\sin\psi+S_z\cos\psi \tag{34}$$

with $0\leq\phi\leq 2\pi$ and $0\leq\psi\leq\pi/2$. We have computed the event rates for a detector with a total acceptance $\int S\,d\Omega=6000$ m^{2}sr, and the aspect ratio $S_x+S_y=S_z/2$. These parameters were chosen as realistic estimates of the size of a feasible detector, being close to the size of the planned MACRO detector in the Gran Sasso Laboratory.[15] The resulting rates are

$$R_{\mu^-}(0° \leq \psi \leq 60°)\simeq 150\ \text{events/yr}\ , \tag{35}$$

$$R_{\mu^-}(60° \leq \psi \leq 90°)\simeq 132\ \text{events/yr}\ , \tag{36}$$

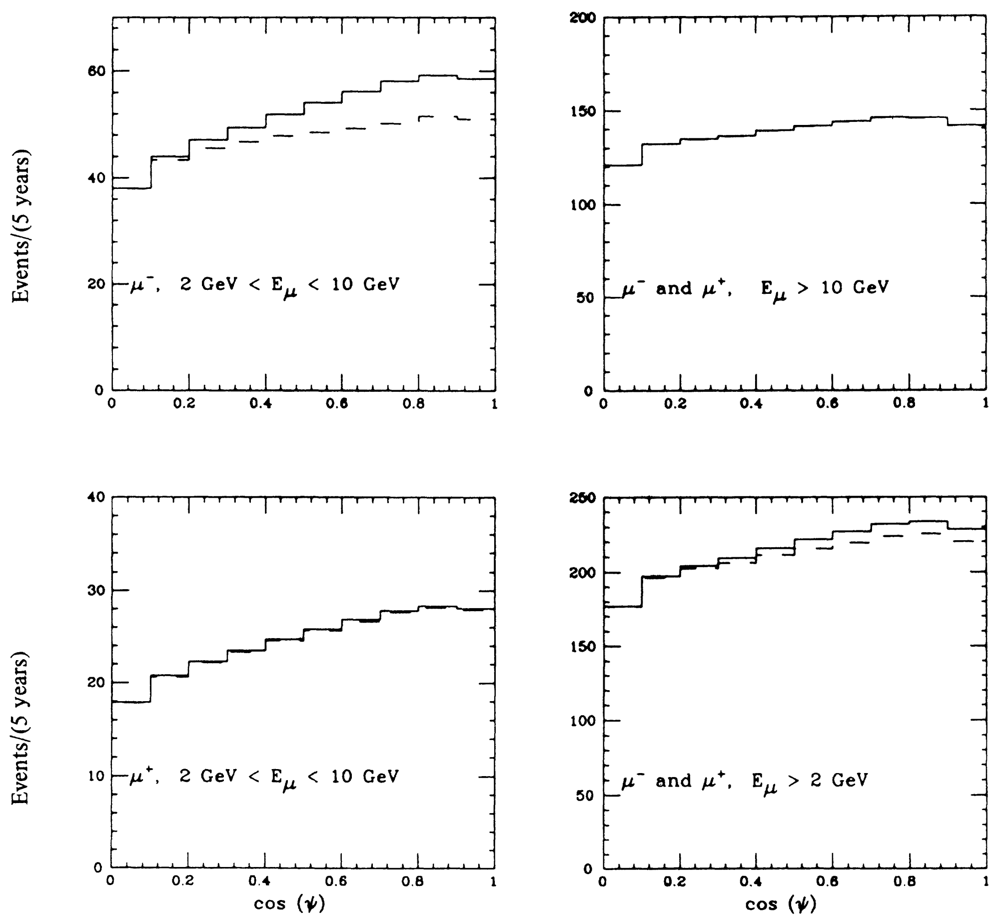

FIG. 9. Effect of neutrino oscillations for the choice of parameters $\sin^2 2\theta=0.04$ and $\Delta m^2=3\times 10^{-3}$ eV^2 in the data that a large underground detector is expected to collect in 5 yr of running. We assumed that μ's of different charges can be separated below $E_\mu=10$ GeV. In (a) the μ^- data show a clear depression with respect to the rate expected without neutrino oscillations (dashed line); in (b) the μ^+ data show no oscillation signal, in (c) the high-energy ($E_\mu \geq 10$ GeV) μ^- and μ^+ data are also insensitive to oscillations.

$$R_{\mu^+}(0^\circ \le \psi \le 60^\circ) \simeq 74 \text{ events/yr} , \tag{37}$$

$$R_{\mu^+}(60^\circ \le \psi \le 90^\circ) \simeq 65 \text{ events/yr} . \tag{38}$$

V. EFFECT OF NEUTRINO OSCILLATIONS

Neutrino oscillations reduce the flux of upward muons. The reduction will depend on the parameters of neutrino mixing Δm^2 and $\sin^2 2\theta$ and on the energy and direction of the muon. It is straightforward to obtain the differential upward muon flux for any choice of the oscillation parameters.

In Fig. 7 we show, after integrating over nadir angles $0^\circ \le \psi \le 60^\circ$, the differential spectrum of the muons detected in the model of apparatus described in the previous section, for a fixed value of the mixing angle $\sin^2 2\theta = 0.04$, that corresponds to the Cabibbo angle, and different values of Δm^2. The qualitative features of the reduction can be easily understood. For each value of Δm^2, neutrinos in the two narrow bands of energy (15) and (16) are "rotated away" to the other flavor. However, a μ of energy E_μ will be produced by a distribution of neutrino energy $[E_\nu \simeq (1-10)E_\mu]$ (cf. Fig. 8). The effect is, therefore, diluted, and is present as a reduction of the order of $\sim 20\%$ spread over a larger band of energies.

VI. EXPERIMENTAL CONSIDERATIONS

It is clear from the discussion in the previous paragraph that a measurement of the charge of the muons would be highly desirable. Such a measurement is technically feasible. For example, a conceivable underground neutrino-oscillation detector could include one or more layers of magnetized iron. For μ's below a certain momentum, the charge would be deduced by the deflection of μ's in the magnetic field. For instance we could think of using two layers of magnetized iron, one parallel to the plane (x,y), which could provide the horizontal field and a vertical plane for the charge separation of the nearly horizontal muons.

The deflection of a muon will be given by the formula

$$\Delta\psi = \frac{eB_{\text{sat}}\delta_F}{p_\mu \cos\psi} , \tag{39}$$

δ_F being the iron thickness and B_{sat} its saturation field. The spread induced by the multiple scattering will be

$$\sigma_{\text{scatt}} = \frac{1}{\sqrt{3}} \frac{0.0141}{p_\mu \cos\psi} \left[\frac{\delta_F}{L_R \cos\psi} \right]^{1/2} , \tag{40}$$

where L_R is the radiation length for iron. The ratio of

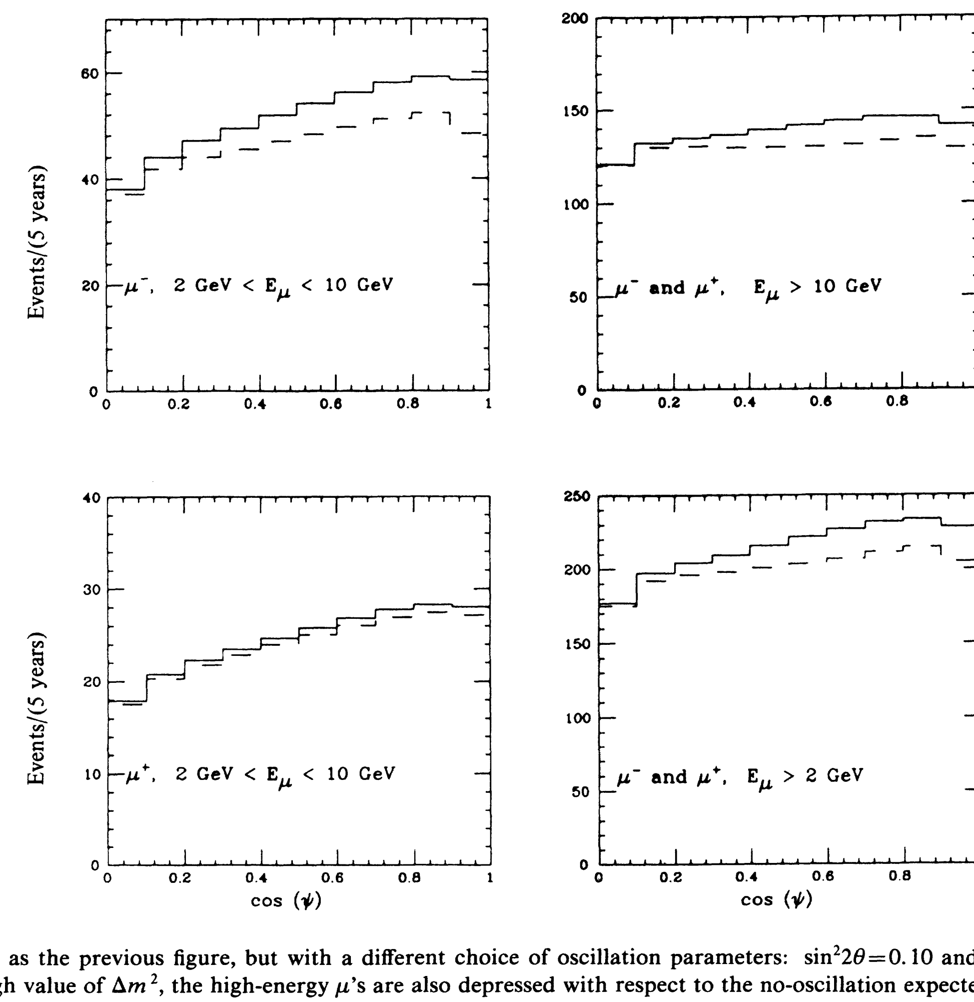

FIG. 10. Same as the previous figure, but with a different choice of oscillation parameters: $\sin^2 2\theta = 0.10$ and $\Delta m^2 = 10^{-2}$ eV^2. Because of the high value of Δm^2, the high-energy μ's are also depressed with respect to the no-oscillation expected rate.

the deflection $\Delta\psi$ due to the magnetic field to the dispersion due to multiple scattering is independent from the momentum of the muons and increase $\sim\sqrt{\delta_F}$. In order to select the charge of the muons we should have $2\Delta\psi > 3\sigma_{\mathrm{scatt}}$. If we consider about 20 cm of iron driven to the saturation point ($B_{\mathrm{sat}} \simeq 20$ kG), formula (39) gives $\Delta\psi \simeq 120$ mrad$/(p_\mu \cos\psi)$. The angular resolution σ_{track} of a muon's tracking system can easily be in the range of 2–5 mrad. Therefore, we can expect to be able to separate charges up to 15–40 GeV. The resolution in the measurements of the momentum will be

$$\Delta p_\mu / p_\mu^2 \propto \sqrt{\sigma_{\mathrm{scatt}}^2 + \sigma_{\mathrm{track}}^2}\ ,$$

and, therefore, in our case is dominated by the multiple scattering below 15–20 GeV where we estimate $\Delta p/p \simeq 0.4$. Above this limit the momentum resolution will be limited by the tracking accuracy, then we have $\Delta p/p \sim 0.03p$ (p in GeV). This rough momentum measurement could, however, also be very useful in the search for an oscillation signal.

In the light of the discussion outlined above, we have assumed that with the present technology a muon under-

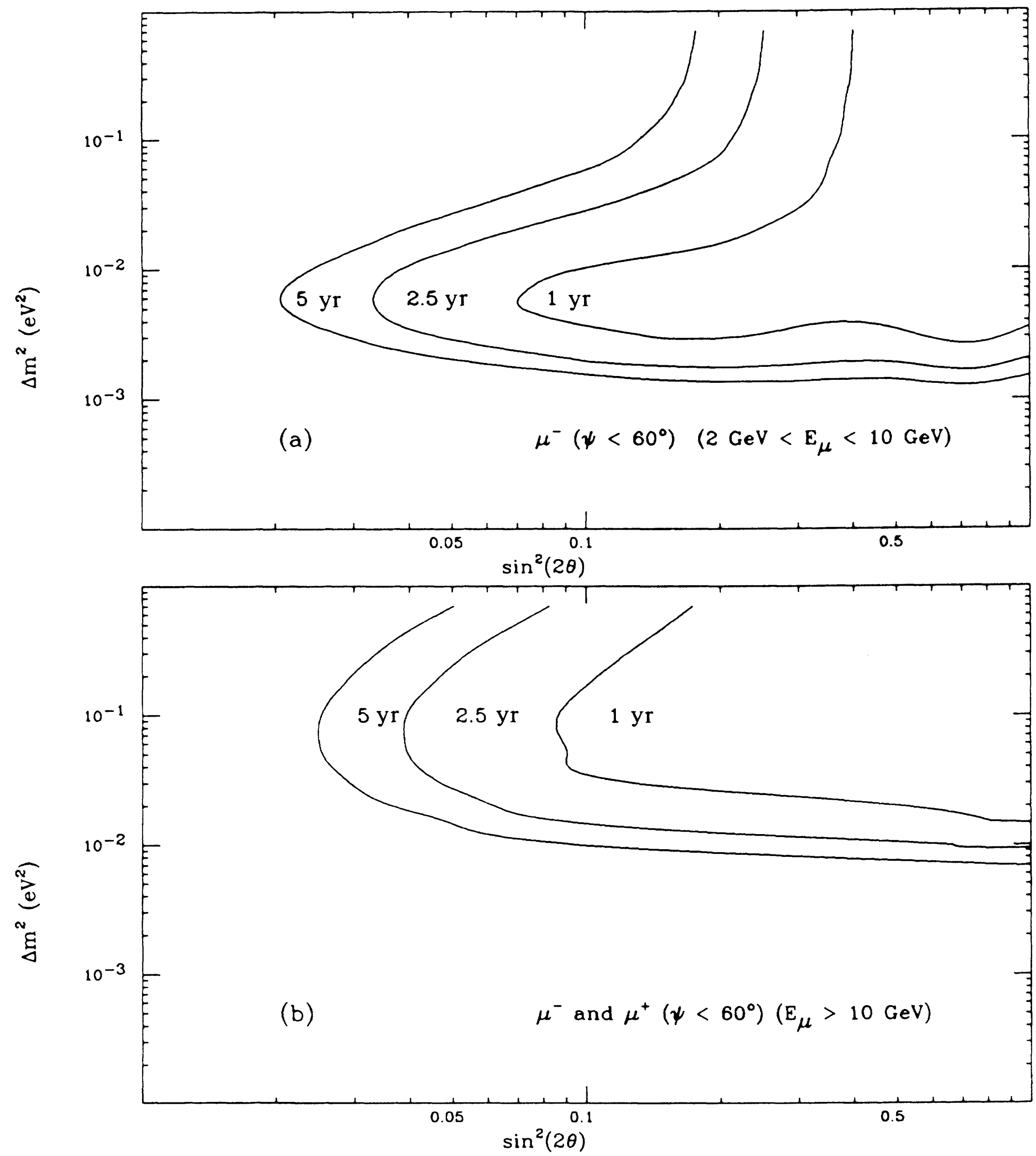

FIG. 11. Region in the parameter space (Δm^2,$\sin^2 2\theta$) that could be excluded at 90% C.L. in a given amount of running time with the underground muon detector described in the text. (a) shows the limits that could be obtained by studying the rate of the low-energy (2 GeV $\le E_\mu \le$ 10 GeV) μ^-'s. (b) shows the limits achievable without a charge measurement. In both figures systematic uncertainties have not been taken into account.

ground detector could conservatively separate the charges of upward-going muons in the range 2–10 GeV, and we have investigated the sensitivity to neutrino oscillations of an underground detector as the one previously described.

The possible results of five years of running are shown in Fig. 9. The detected upward-muons have been divided into three categories: high-energy ($E_\mu > 10$ GeV) μ's whose charge is not determined, low-energy μ^- (2 GeV $\leq E_\mu \leq 10$ GeV), and low-energy μ^+. The angular distributions for each of the three categories and the sum are plotted, comparing the expected result with no oscillations, with the result, assuming for the oscillation parameters the values $\Delta m^2 = +3\times 10^{-3}$ eV^2 and $\sin^2 2\theta = 0.10$. The low-energy μ^- signal shows a clear reduction due to oscillations. The low-energy μ^+ is left essentially unchanged. In this case also the high-energy part of the detected muon spectrum is unchanged. Without the determination of the charge, the experimenters would only have available the last distribution, which sums over all muons charge and energies. A statistically significant oscillation signal is actually present also in the cumulative distribution; however, the uncertainty in the normalization of the no-oscillation curve would probably wash out the signal. The separation of the muon charges not only enhances the statistical significance of the signal, but gives a powerful handle to control this systematic uncertainty, allowing the use of the nonmodulated μ^+ flux as an absolute reference. The separation of the muon signal in two (or possibly more) momentum bins is also very helpful, because the oscillation signal, as discussed before is important only in a limited range of E_μ and the comparison of the relative normalization of the different momentum bins would be an additional consistency check for the experimenters. A larger value for the mass splitting Δm^2, as shown in Fig. 10, would produce a depression of the μ^- flux for larger energies.

To estimate the sensitivity of this detector to neutrino oscillations, we have computed the rate of μ^- in the energy region (2 GeV $\leq E_\mu \leq 10$ GeV) and the angular region ($0° \leq \psi \leq 60°$) for different values of the oscillation parameters, and compared the result with the rate without oscillations. Assuming perfect knowledge of the expected flux with no oscillations, a fixed exposure time (1, 2.5, and 5 yr) would allow us to eliminate with 90% confidence level the regions shown in Fig. 11. In the same figure we show the region excluded comparing the cumulative rate [μ^- and μ^+ with ($E_\mu \geq 2$ GeV)] with the total expected rate without oscillations. It should be stressed that the assumption that the sensitivity is dominated by statistics, in the latter case is not realistic.

In Fig. 12 we compare the results given above with the present experimental limits obtained from accelerator (curve a) or reactor (curve b) experiments, together with the region (curve f) of the parameter space[16] that would explain the reduced neutrino capture rate observed by the Davis experiment as a resonant neutrino oscillation in the Sun, and the region that could be excluded from the study of contained atmospheric neutrino interactions in the IMB experiment (curve e), as discussed in Ref. 17.

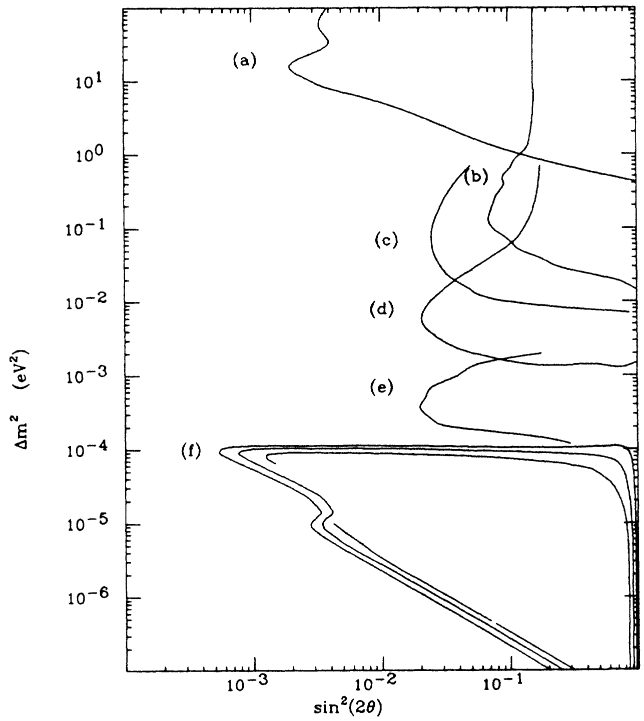

FIG. 12. Compares the limits achievable with the method discussed in this paper [curves (c) and (d)] with the existent experimental limits obtained from accelerators [curve (a)] and reactors [curve (b)]; the limits obtainable from experiments that also use the atmospheric neutrino flux, but study contained neutrino interactions as discussed in Ref. 17 (curve e); and the region of parameter space that would explain the reduced neutrino flux observed by the Davis experiment as resonant oscillations in the Sun (curve f), after Ref. 16.

VII. CONCLUSIONS

The Wolfenstein-Mikheyev-Smirnov matter effect is of crucial importance in the analysis of experiments searching for ($\nu_\mu \leftrightarrow \nu_e$) oscillations using atmospheric neutrinos. For small mixing angles the signature of neutrino oscillations would be a reduction of the μ^- flux (for $\Delta m^2 < 0$) or the μ^+ flux (for $\Delta m^2 < 0$). The reduction of the flux is important only for a limited range of muon energies:

$$E_\mu \simeq (0.5-3) \left[\frac{|\Delta m^2|}{10^{-3}\ \text{eV}^2} \right] \text{GeV} . \tag{41}$$

Integrating over all energies and summing over the μ^+ and μ^- signals would dilute the statistical significance of an oscillation signal. The sensitivity of one experiment would, however, be limited by systematic difficulties, associated with the knowledge of the flux without oscillations.

An experimental setup that could measure the charge of the μ's, and, with very poor resolution, the muon momentum, would dramatically improve the sensitivity of one experiment. The statistical significance of the signal would be enhanced because it could be looked for in a more limited region dividing the total rate according to charge, and one or more momentum bins. Still more importantly, a measurement of the muon charge would reduce considerably the systematic uncertainty due to the poor knowledge of the absolute normalization of the neutrino flux. An oscillation signal should be looked for when comparing the μ^- and μ^+ flux and also, when comparing the low-energy and high-energy parts of the μ^- and μ^+ flux. The charge and momentum measurement needed for this improvement in sensitivity appears feasible. The improved detector, could explore the region of mixing angles $\sin^2 2\theta \geq 0.02$. Assuming a minimum detectable muon energy $E_{\mu\ \min} = 2$ GeV, the detector would be sensitive to mass differences $\Delta m^2 \geq 3\times 10^{-3}$ eV^2. Sensitivity to lower muon energies would improve the limit on Δm^2. The method of studying the upward muon flux is complementary to the method of studying the up/down asymmetry of contained neutrino interactions. This last method is mostly sensitive to lower neutrino energies and, therefore, to lower values of the parameter Δm^2.

In these considerations we are assuming that good theoretical control of the ratios $\nu_\mu/\bar{\nu}_\mu$ and $\nu_e/\bar{\nu}_e$ and of their variation with energy and angle is possible. A detailed study of this problem is needed. More precise measurements of the ratio μ^+/μ^- could be useful in this study.

ACKNOWLEDGMENTS

We are grateful to B. Barish, M. Lusignoli, P. Pistilli, and T. K. Gaisser for stimulating discussions on the problems discussed in this paper. We wish also to thank T. P. Walker for providing the data reported in Fig. 12 in tabular form.

[1]B. Pontecorvo, Zh. Eksp. Teor. Fiz. **7**, 172 (1958) [Sov. Phys. JETP **34**, 247 (1958)].

[2]See, e.g., J. M. LoSecco *et al.*, in *Neutrino '86, Neutrino Physics and Astrophysics,* proceedings of the Twelfth International Conference, Sendai, Japan, 1986, edited by T. Kitagaki and H. Yuta (World Scientific, Singapore, 1986).

[3]See D. S. Ayres *et al.*, Phys. Rev. D **15**, 902 (1984), and references therein.

[4]L. Wolfenstein, Phys. Rev. D **17**, 2369 (1978).

[5]S. P. Mikheyev and A. Yu. Smirnov, Yad. Fiz. **42**, 1441 (1985) [Sov. J. Nucl. Phys. **42**, 913 (1985)].

[6]H. A. Bethe, Phys. Rev. Lett. **56**, 1305 (1986); E. W. Kolb, M. S. Turner, and T. P. Walker, Phys. Lett. B **175**, 478 (1986); S. P. Rosen and J. M. Gelb, Phys. Rev. D **34**, 969 (1986).

[7]J. N. Bahcall, Rev. Mod. Phys. **50**, 881 (1978).

[8]F. D. Stacey, *Physics of the Earth* (Wiley, New York, 1969), p. 281.

[9]L. Maiani, in *Proceedings of the International Symposium on Lepton and Photon Interactions at High Energies,* Hamburg, 1977, edited by F. Gutbrod (DESY, Hamburg, 1977), p. 867.

[10]M. Gell-Mann, P. Ramond, and R. Slansky, in *Supergravity,* edited by P. van Nieuwenhuizen and D. Z. Freeman (North-Holland, Amsterdam, 1979).

[11]T. K. Kuo and J. Pantaleone, Phys. Rev. Lett. **57**, 1805 (1986).

[12]L. V. Volkova, Yad. Fiz. **31**, 1510 (1980) [Sov. J. Nucl. Phys. **31**, 784 (1980)].

[13]T. K. Gaisser and T. Stanev, Phys. Rev. D **30**, 985 (1984).

[14]D. W. Duke and J. F. Owens, Phys. Rev. D **30**, 49 (1984).

[15]J. L. Stone, in *Proceedings of the 19th International Cosmic Ray Conference,* La Jolla, California, 1985, edited by F. C. Jones, J. Adams, and G. M. Mason (NASA Conf. Publ. No. 2376) (Goddard Space Flight Center, Greenbelt, MD, 1985), Vol. 8, p. 226.

[16]S. J. Parke and T. P. Walker, Phys. Rev. Lett. **57**, 2322 (1986); **57**, 3124(E) (1986).

[17]E. D. Carlson, Phys. Rev. D **34**, 1454 (1986).